

## Direct Current Control of Three Magnon Scattering Processes in Spin-Valve Nanocontacts

H. Schultheiss,<sup>1</sup> X. Janssens,<sup>2</sup> M. van Kampen,<sup>2</sup> F. Ciubotaru,<sup>1</sup> S. J. Hermsdoerfer,<sup>1</sup> B. Obry,<sup>1</sup> A. Laraoui,<sup>1</sup> A. A. Serga,<sup>1</sup> L. Lagae,<sup>2</sup> A. N. Slavin,<sup>3</sup> B. Leven,<sup>1</sup> and B. Hillebrands<sup>1</sup>

<sup>1</sup>Fachbereich Physik and Forschungszentrum OPTIMAS, Technische Universität Kaiserslautern, 67663 Kaiserslautern, Germany

<sup>2</sup>IMEC, Kapeldreef 75, 3001 Leuven, Belgium

<sup>3</sup>Department of Physics, Oakland University, Rochester, Michigan 48309, USA

(Received 5 May 2009; revised manuscript received 28 July 2009; published 8 October 2009)

We have investigated the generation of spin waves in the free layer of an extended spin-valve structure with a nanoscaled point contact driven by both microwave and direct electric current using Brillouin light scattering microscopy. Simultaneously with the directly excited spin waves, strong nonlinear effects are observed, namely, the generation of eigenmodes with integer multiple frequencies ( $2f$ ,  $3f$ ,  $4f$ ) and modes with noninteger factors ( $0.5f$ ,  $1.5f$ ) with respect to the excitation frequency  $f$ . The origin of these nonlinear modes is traced back to three-magnon-scattering processes. The direct current influence on the generation of the fundamental mode at frequency  $f$  is related to the spin-transfer torque, while the efficiency of three-magnon-scattering processes is controlled by the Oersted field as an additional effect of the direct current.

DOI: 10.1103/PhysRevLett.103.157202

PACS numbers: 75.40.Gb, 75.40.Mg, 75.75.+a, 85.75.-d

Magnetic excitations generated by a high-density electric current in a ferromagnetic nanostructure have attracted growing attention due to the importance of understanding the physical mechanisms responsible for the excitation process. The discovery of the spin transfer torque (STT) effect in 1996 by Slonczewski [1] and Berger [2], i.e., the excitation of the precession of the magnetization in ferromagnetic thin films and nanostructures by a spin polarized direct electric current, has offered a new scheme for spin-wave excitation in magnetic nanostructures. In a point contact structure, this torque may excite spin waves whose frequencies are tunable via both current and applied magnetic field [3,4]. The electrical contacts made with diameters less than 100 nm to a continuous spin-valve multilayer stack permit one to achieve large current densities with relatively small applied currents. If the current density is large enough, the STT compensates the natural dissipation processes. This may lead to self-sustained dynamics under and near the point contact such as the formation of nonlinear evanescent bullet modes in the case of in-plane magnetization [5,6]. The impact on spin waves by a microwave current flowing through a point contact was demonstrated [7,8], with possible applications in, e.g., radio-frequency devices for wireless communication.

In this Letter we report on the instability of artificially generated spin waves in spin-valve nanocontacts, where the excitation density for the magnetization dynamics is crossing a limit not reached so far. As a result the spin-wave system is driven to amplitudes far beyond the linear regime, and nonlinear processes are observed such as the splitting and the confluence of spin waves. Experiments with additionally applied direct currents allowed us to trace back the point of origin of these nonlinear spin waves to the interior of the nanocontact. Moreover, it is demonstrated that the power thresholds and frequencies for these non-

linear processes are largely changed over a wide range by the application of a direct current.

The investigated structures consist of an extended spin-valve multilayer sequence [IrMn(6 nm)/Co<sub>90</sub>Fe<sub>10</sub>(5 nm)/Cu(3.5 nm)/Ni<sub>80</sub>Fe<sub>20</sub>(7 nm)/Pt(3 nm)] with lateral dimensions of  $15 \times 45 \mu\text{m}^2$ . The electric current is injected through a nanoscaled metallic point contact on top of the spin valve. The Ni<sub>80</sub>Fe<sub>20</sub> layer acts as the magnetic free layer of the spin valve and the Co<sub>90</sub>Fe<sub>10</sub> layer, which is pinned by an antiferromagnetic layer (IrMn), serves as a reference layer for the giant magnetoresistance measurements. A detailed description of the sample characteristics is given in [9]. Figure 1 shows a scheme of the sample geometry and scanning electron microscopy (SEM) images of the point contact. A feature of the investigated structure is the triangularly shaped top electrode. This configuration provides optical access to a large part of the magnetic area and enables the investigation of the magnetization dynamics close to the nanocontact with

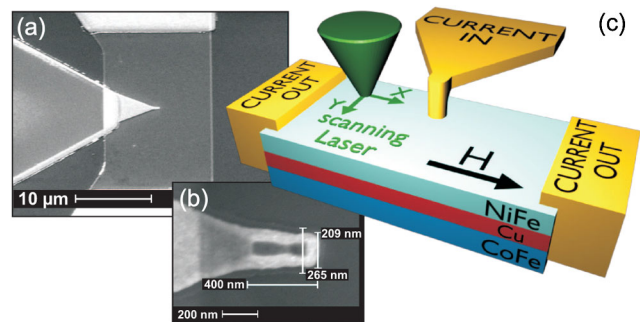


FIG. 1 (color online). SEM images of the sample (a) and of the top electrode (b). (c) Schematic representation of the sample with focused light near the point contact in the presence of an external in-plane bias magnetic field  $H$ .

Brillouin light scattering microscopy. This technique uses a focused laser spot to probe the spin waves with a spatial resolution of 250 nm and a frequency resolution of up to 50 MHz [10,11].

In the experiments reported here the free layer is saturated by an external magnetic field  $H$  applied in the plane of the magnetic layer, along to the long axis of the spin-valve stack [Fig. 1(c)] and antiparallel to the pinned  $\text{Co}_{90}\text{Fe}_{10}$  layer. Spin waves were excited in the structure by applying a microwave current with various frequencies (2 to 12 GHz) and powers (0.1 to 20 mW). Using a bias-tee, an additional direct current was injected. Typical current densities used in our experiments do not exceed  $3 \times 10^{11}$  A/m to avoid destruction of the tip shaped top electrode. This is a factor of 2 smaller than the critical current density required for spin torque driven steady state oscillations in similar devices without optical access. In the first step the dynamic response of the device was characterized as a function of the applied frequency in order to determine the resonance frequencies of the  $\text{Ni}_{80}\text{Fe}_{20}$  layer close to the point contact. The results are shown in Figs. 2(a) and 2(b) for externally applied fields of 10.297 kA/m (129.4 Oe) and 19.783 kA/m (248 Oe), respectively. The output power of the microwave source was 10 mW. These intensity graphs display the measured Brillouin light-scattering (BLS) intensity in a color code as a function of the micro-

wave excitation frequency ( $x$  axis) and the frequency position in the BLS spectrum ( $y$  axis). The diagonal in the figure represents the efficiency of the excitation of spin waves with frequencies that match the applied microwave frequency  $f$ . Simultaneously with the directly excited spin waves, strong nonlinear effects appear, namely, the generation of modes with integer multiple frequencies ( $2f$ ) and modes with noninteger factors ( $0.5f$ ) with respect to the excitation frequency. With a further increasing of microwave output power the spin-wave irradiation at combination frequencies  $1.5f$ ,  $3f$ , etc., are observed [12].

The excitation of these nonlinear modes can be understood within the framework of three-magnon scattering processes [13] in which the total energy and momentum are conserved. The white arrows in Fig. 2(a) show directly the conservation of the energy in those processes. In the case of confluence, two magnons with frequency  $f$  combine into a single magnon with doubled frequency  $2f$  [process 1 in Fig. 2(a)]. In the other case, one magnon with frequency  $f$  splits in two magnons, each one having half the frequency  $f/2$  (process 2). From Figs. 2(a) and 2(b) it is evident that the splitting process does not appear below a certain threshold frequency [white circles in Figs. 2(a) and 2(b)], which depends on the applied field. With an increasing magnetic field this threshold frequency increases as well from approximately 3.2 GHz for  $H = 10.297$  kA/m (129.4 Oe) to 4.5 GHz for  $H = 19.783$  kA/m (248 Oe).

This threshold frequency can be derived from the analytical dispersion relations of spin-wave eigenmodes [14]. We calculated the dispersion relations for a 7 nm thick  $\text{Ni}_{80}\text{Fe}_{20}$  layer and for applied magnetic fields of 10.297 kA/m and 19.783 kA/m and plotted them in Fig. 2(c). We used standard material parameters for the saturation magnetization ( $M_s = 800$  kA/m) and the exchange constant ( $A = 1.3 \times 10^{-11}$  J/m). Note that the dispersion of spin waves in a thin film is strongly anisotropic, depending on the propagation direction of spin waves with respect to the static magnetization vector. For each magnetic field, the upper (lower) curve corresponds to spin waves propagating perpendicular (parallel) to the magnetization vector. These two extremal dispersion curves define the frequency band in which spin-wave eigenmodes are allowed. Therefore, taking energy conservation into account, it is expected that a splitting process can occur only if the excitation frequency is at least twice the frequency at the bottom of the spin-wave band. The observed threshold frequencies for the  $f/2$  modes match the frequency at the bottom of the spin-wave band [white circles in Fig. 2(c)]. This supports the interpretation of three-magnon splitting as the responsible mechanism for the generation of the  $f/2$  modes.

Since the splitting of magnons is a nonlinear process, the amplitudes of the excited spin-wave modes ( $f$  and  $f/2$ ) were studied as a function of the applied microwave power

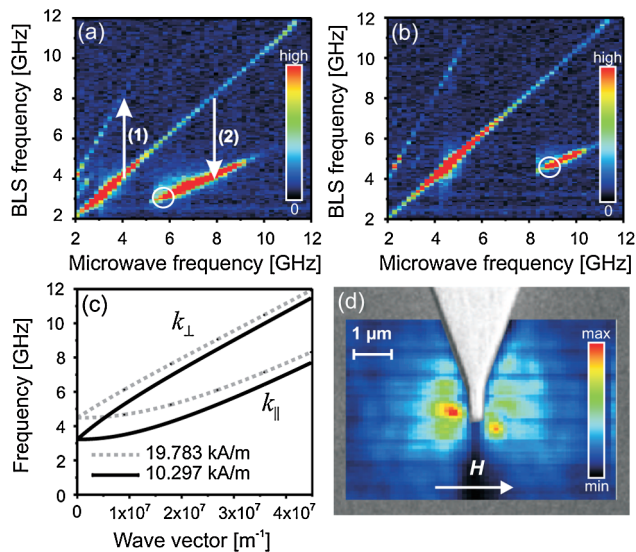


FIG. 2 (color online). Spin-wave amplitudes measured with Brillouin light-scattering microscopy as a function of the RF excitation frequency ( $x$  axis) and the position in the Brillouin light-scattering spectrum ( $y$  axis) for an in-plane magnetic field of (a) 10.297 kA/m (129.4 Oe) and (b) 19.783 kA/m (248 Oe) [12]. (c) Spin-wave dispersion band for the magnetic fields corresponding to panels (a) and (b). The top and bottom branches correspond to wave vectors oriented perpendicular and parallel to the magnetic field. (d) BLS-microscopy image of the two-dimensional distribution of the spin waves radiated from the contact at a pumping frequency of 3.1 GHz.

[Fig. 3(a)]. The excitation frequency is fixed at 8.9 GHz, just above the threshold frequency which was found for the splitting process in Fig. 2(b). As expected, the amplitude of the directly excited spin waves increases linearly with the applied microwave power. The  $f/2$  mode, however, shows a very different dependency. Starting from very low microwave powers it cannot be detected over a wide range. Upon crossing a certain threshold power, the amplitude increases drastically, and even overcomes the amplitude of the directly excited spin waves. This threshold behavior is characteristic for three-magnon-scattering processes.

The absolute value of the threshold power for the splitting of magnons is a function of many parameters [13]. Most important for the studies presented here is the magnitude of the internal magnetic field and the damping parameter of the spin waves. Since it is well known that spin transfer torque can compensate the natural damping of spin waves, it is of particular interest to investigate the influence of a spin polarized direct current on the  $f$  and  $f/2$  modes. In the experimental geometry a positive polarity of the direct current corresponds to a flow of electrons from the fixed layer to the free layer. For a fixed applied microwave power, the amplitude of the  $f$  mode was measured as a function of the direct current. Demokritov *et al.* showed in [15] that the Gilbert damping parameter  $\alpha$  is proportional to the inverse square root of the BLS intensity. Following their analysis with the experimental results reported here a decrease of  $\alpha$  was observed with increasing direct current [Fig. 3(b)], consistent with the STT effect. Note that in Fig. 3(b) the values of  $\alpha$  are normalized to the case of zero applied current.

Furthermore, a strong influence of the direct current on the power dependency of the splitting processes was observed and is shown in Fig. 4(a). The threshold power for the excitation of the  $f/2$  mode is growing by orders of magnitude with rising direct currents. Figure 4(b) shows the threshold powers as a function of the direct current for two values of the applied magnetic field [19.5 kA/m (245 Oe) and 22.4 kA/m (281 Oe)]. A nonlinear relation

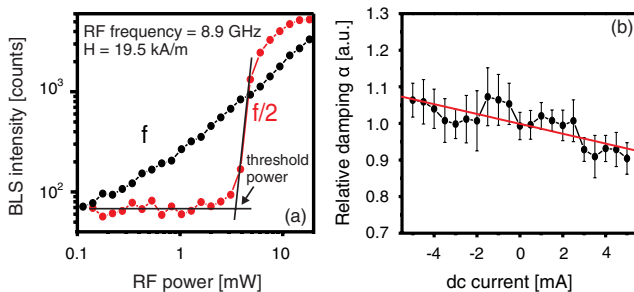


FIG. 3 (color online). (a) BLS intensity of the  $f$  and  $f/2$  modes as a function of microwave excitation power ( $x$  axis). The indicated point represents the threshold power for the  $f/2$  mode. (b) Relative damping of the directly excited spin waves at 8.9 GHz as a function of the direct current. The straight line represents the best linear fit of the data.

between the threshold power and the direct current is apparent. From theory it is known that the STT effect causes a linear relation between  $\alpha$  and the direct current [1,16], leading to a linear response of the threshold power as a function of the current strength. Obviously, this linear behavior is not observed in the experimental data presented here. Moreover, the increase of the threshold power with increasing direct current suggests that the internal damping is getting larger as well. These results are in contradiction with a STT-based mechanism.

So far the influence of the Oersted field created by the direct current was not addressed. An additional magnetic field created by the current will change the dispersion relation of the spin waves. In particular, it will modify the frequency at the bottom of the spin-wave band. For this reason, the connection between the threshold frequency of the  $f/2$  mode and the magnitude of the direct current as well as the distance to the point contact was studied. The results, plotted in Fig. 4(c), show that the direct current induces a proportional shift of the threshold frequency of the  $f/2$  mode, very similar to the results produced by changing the applied magnetic field [Figs. 2(a) and 2(b)]. We determined the contribution of the Oersted field by adding an additional magnetic field to the dispersion relation. This field is chosen so that the bottom frequency of the spin-wave band matches the threshold frequency observed experimentally in Fig. 4(c). This analysis yields an additional magnetic field of

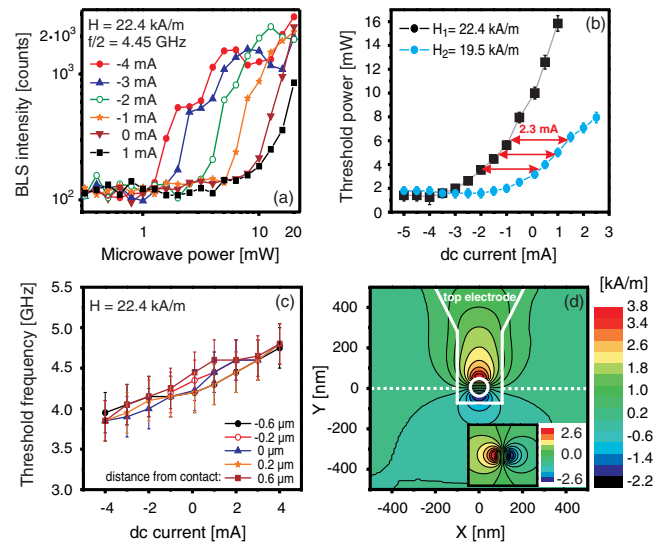


FIG. 4 (color online). (a) Generation efficiency of the  $f/2$  mode ( $=4.45$  GHz) as a function of the applied microwave power for different direct currents ( $H = 22.4$  kA/m). (b) Extracted threshold power for the  $f/2$  mode over the direct current for two values of the applied field. (c) Influence of the scan position on the threshold frequency over the direct current for 20 mW. (d) Spatial distribution of the Oersted field components parallel and perpendicular (inset) to the applied field. The inset figure has a lateral size of  $300 \text{ nm} \times 300 \text{ nm}$ .

1.27 (kA/m)/mA (16 Oe/mA) created by the direct current.

Using a micromagnetic simulation software [17] the current distribution and the corresponding Oersted field were simulated in the free layer with and without the contribution of the top electrode, respectively. It was found that the triangular lead induces an asymmetric magnetic field caused by the Oersted field of the flowing direct current, as can be seen in Fig. 4(d). This additional magnetic field is proportional to the applied direct current. A contribution of 1.2 (kA/m)/mA ( $\sim 15$  Oe/mA) parallel to the externally applied field was found from the simulations. This value is in very good agreement with the magnetic field that we used to match the spin-wave dispersion to the obtained experimental results in Fig. 4(c). Thus, for different currents the  $f/2$  mode is excited at a different position in the spin-wave band. From bulk spin-wave theory it is known that the threshold for magnon splitting processes strongly depends on the direction of the wave vectors of the created magnons [13]. For magnons created at the bottom of the spin-wave spectrum, where the wave vector is parallel to the magnetization, the efficiency of these splitting processes should be zero. In the ultrathin magnetic films investigated here the efficiency is nonzero for these processes because of the strong shape anisotropy. Above the bottom of the spin-wave spectrum the efficiency for the splitting increases and, therefore, the threshold power decreases because magnons with a wave vector not parallel to the magnetization start to participate in the splitting processes. However, up to now there is no theory for magnon splitting processes in ultrathin magnetic films which we could use for a quantitative comparison with our experimental results. Hence, the inhomogeneous magnetic field within the nanocontact area is responsible for the behavior of the frequency and power thresholds of the  $f/2$  mode when the direct current is changed. Note that in Fig. 4(b) the threshold powers for the generation of the  $f/2$  mode for the magnetic fields  $H_1$  and  $H_2$  are shifted by a constant value of 2.3 mA with respect to each other. This current difference corresponds to a magnetic field of 2.9 kA/m (36 Oe) using the calibration factor 1.27 (kA/m)/mA (16 Oe/mA) for the Oersted field created by the direct current. This value matches well the difference  $\Delta H = H_1 - H_2$  in both applied magnetic fields.

Clear evidence for the generation of the  $f/2$  mode just near the contact area arises from the measurements made for different scan positions along the dashed white lines indicated in Fig. 4(d). The results for different positions shown in Fig. 4(c) prove that the threshold frequency does not depend on the distance from the contact. Moreover, the threshold power for the  $f/2$  mode does not depend on the scan position. These results suggest that the Oersted field

created outside the contact, which is strongly position dependent, has no contribution to the splitting process of the magnons. The magnons with half the excitation frequency are generated inside the contact area. Because of the very low group velocity of spin waves close to the bottom of the spin-wave band the  $f/2$  mode remains localized close to the nanocontact.

In conclusion, the magnetization dynamics in a spin-valve nanocontact has been investigated under the influence of an microwave and direct current by means of Brillouin light scattering microscopy. The large current densities that can be achieved in a nanocontact allow the excitation of spin waves in the nonlinear regime. In the presence of a direct current the efficiency of the excitation of spin waves can be enhanced or reduced due to the spin transfer torque effect. The experimental results reported here show that magnon splitting and confluence processes take place within the nanocontact. The threshold properties of spin waves with half the excitation frequency are controlled by the Oersted field created by the current within the point contact and due to the Oersted field contribution of the asymmetric top electrode.

This work was supported by the European Commission within the EU-MRTN SPIN SWITCH (MRTN-CT-2006-035327) and by the Deutsche Forschungsgemeinschaft within the SPP1133.

- 
- [1] J. C. Slonczewski, *J. Magn. Magn. Mater.* **159**, L1 (1996).
  - [2] L. Berger, *Phys. Rev. B* **54**, 9353 (1996).
  - [3] Y. Ji *et al.*, *Phys. Rev. Lett.* **90**, 106601 (2003).
  - [4] W. H. Rippard *et al.*, *Phys. Rev. Lett.* **92**, 027201 (2004).
  - [5] A. N. Slavin and V. S. Tiberkevich, *Phys. Rev. B* **72**, 092407 (2005).
  - [6] G. Consolo *et al.*, *Phys. Rev. B* **76**, 144410 (2007).
  - [7] W. H. Rippard *et al.*, *Phys. Rev. Lett.* **95**, 067203 (2005).
  - [8] S. H. Florez *et al.*, *Phys. Rev. B* **78**, 184403 (2008).
  - [9] Q. Mistral *et al.*, *Phys. Rev. Lett.* **100**, 257201 (2008).
  - [10] V. E. Demidov *et al.*, *Appl. Phys. Lett.* **90**, 172508 (2007).
  - [11] V. E. Demidov *et al.*, *Appl. Phys. Lett.* **85**, 2866 (2004).
  - [12] See EPAPS Document No. E-PRLTAO-103-002943 for auxiliary images. A direct link to this document may be found in the online article's HTML reference section. For more information on EPAPS, see <http://www.aip.org/pubservs/epaps.html>.
  - [13] A. G. Gurevich and G. A. Melkov, *Magnetization Oscillations and Waves* (CRC, Boca Raton, FL, 1996).
  - [14] B. A. Kalinikos and A. N. Slavin, *J. Phys. C* **19**, 7013 (1986).
  - [15] S. O. Demokritov and V. E. Demidov, *IEEE Trans. Magn.* **44**, 6 (2008).
  - [16] S. I. Kiselev *et al.*, *Nature (London)* **425**, 380 (2003).
  - [17] LLG Micromagnetics developed by M. R. Scheinfein.